Konne et al., J Material Sci Eng 2017, 6:5
DOI: 10.4172/2169-0022.1000385

Journal of Material Sciences & Engineering

Research Article **Open Access**

Demetallization of Nickel from Crude Oil using Aluminum Oxide (Al_2O_3) Nanoparticles Synthesized with Sodium Dodecyl Sulfate (SDS)

Konne LJ*, Iheanetu UD and Cookey AG

Department of Chemistry, Faculty of Science, Rivers State University, Nkpolu-Oroworukwo Port Harcourt, Nigeria

Abstract

Aluminum oxide nanoparticles (Al_2O_3+SDS and Al_2O_3) were synthesized by a simple sol-gel method for demetallization of nickel from crude oil-water mixture in a batch adsorption process for the first time. The samples were dried, calcined at 550°C, cooled and characterized using scanning electron microscopy (SEM), Energy dispersive spectroscopy (EDS), and X-ray diffraction (XRD) techniques. The XRD confirmed that Al_2O_3 phase were synthesized with more minor impurities of bauxite and silica in Al_2O_3 without SDS. Particle size estimations were 197 and 183 nm for the Al_2O_3 with and without SDS, respectively. SEM showed larger rectangular porous crystallites and thinner net-like-vertical platy crystallites for the former and later samples respectively while the EDS confirmed the presence of Al and O in them. The batch adsorption showed that the %Removal (%R) of the adsorption process increase gradually with increase in adsorbent from 0.02 to 0.1 g to a maximum at 86.1% for Al_2O_3+SDS but decrease with increase in the adsorbent dosage for Al_2O_3 with %R maximum of 78% at the least (0.02 g) dosage. On the other hand, at constant adsorbent dosage, %R of 94 and 93% for a 1:3 crude oil-water mixture were obtained for Al_2O_3+SDS and Al_2O_3, respectively. This confirmed greater capacity of Al_2O_3+SDS for the removal of Ni^{2+} ions from crude oil over the control.

Keywords: Demetallization; Al_2O_3; Al_2O_3+SDS; Ni^{2+}; Langmuir and Freundlich

Nomenclature

C_o: Initial Ni^{2+}concentration (mg/ml)

C_e: Equilibrium concentration of Ni^{2+} in solution (mg/ml)

K_L: Langmuir constant (l/mg)

K_F: Freundlich constant (mg/g)

K_1: Pseudo first-order adsorption rate constant (l/min)

K_2: Pseudo second-order adsorption rate constant (g/mg min)

M: Weight of adsorbent (g)

n: Freundlich constant gives an indication about the favorability of the adsorption process

q_e: Adsorption capacity at equilibrium (mg of Ni^{2+}/g adsorbate)

q_{max}: Langmuir constant related to the maximum adsorption capacity (mg/g)

q_t: Adsorption capacity at time t (mg of Ni^{2+}/g adsorbate)

%R: PERCENTAGE removal (efficiency of Ni^{2+} removal)

R_L: The essential features of a Langmuir isotherm/dimensionless constant

R^2: Correlation coefficient

T: Contact time (min)

V: Volume of the solution (l)

Introduction

Crude oil (also called petroleum) is the major source of energy and devastating environmental pollution in Nigeria [1,2]. This is because crude oil contains some heavy metals such as lead, nickel, iron, vanadium, cobalt, zinc, etc. Naturally occurring elements in rock formations enter reservoir crude oil by complexing with chlorophyll residues (porphyrin) during migration/formation processes [3]. They are often present in small amounts in mgg^{-1} or ngg^{-1} range yet pose great concern to the petroleum industry and to the environment due to their ability to accelerate corrosion of distillation towers and turbines, poison catalysts by pore clogging, fissure and deform reactors, pollute the environment, upset natural environmental balances, contaminate food, etc. [4,5]. Demetallization, which has to do with the removal of these metal ions, is therefore a statutory process to enhance efficiency in the oil industry. Among the heavy metals found in crude, nickel determination after demetallization is crucial being constituent of catalysts used in refining processes [4].

Some of the techniques employed for demetallization include coking and hydro treatment [6], microwave-chemical method [7] and most recently, the use of metal oxide nanoparticles, Starch Stabilized Magnetic Nanoparticles (SSMNPs) for the removal of nickel from crude oil monitored by UV-Vis spectrophotometry [5]. The UV-V is method reported dissolved 0.2 ml of the filtrate in 10 ml of hexane for analysis. While the previous methods were considered less effective and expensive, the use of SSMNPs with a high efficiency of 93% was quite promising. However, the report recorded some anomalous values at certain concentrations of the starch coating. Similar use of Gama-Al_2O_3 nanoparticles has been applied for the adsorption of asphaltenes from

---

***Corresponding author:** Joshua Lelesi Konne, Department of Chemistry, Faculty of Science, Rivers State University, Nkpolu-Oroworukwo Port Harcourt, Nigeria, Tel: +234 903 885 8167; E-mail: konne.joshua@ust.edu.ng

Received September 18, 2017; **Accepted** October 16, 2017; **Published** October 26, 2017

Citation: Konne LJ, Iheanetu UD, Cookey AG (2017) Demetallization of Nickel from Crude Oil using Aluminum Oxide (Al_2O_3) Nanoparticles Synthesized with Sodium Dodecyl Sulfate (SDS). J Material Sci Eng 6: 385. doi: 10.4172/2169-0022.1000385

heavy oil but not for demetallization target [8]. Some metals could be removed during deasphaltenation by these nanoparticles but not yet investigated.

Aluminum oxide (Al_2O_3) is one of the essential metal oxides because of its broad applications in adsorbents, composite materials and catalyst supports [9,10]. Aluminum oxide (Al_2O_3) nanoparticles could play effective roles in the demetallization of metal ions from crude oil. This is because it has high surface area and catalytic properties. Al_2O_3 nanoparticles do not only adsorb hazardous chemicals but also convert them into smaller and less harmful by-products [11]. In addition, surface modification with surfactants may produce similar enhancement effect reported for starch coated magnetite nanoparticles. Therefore sodium dodecyl sulphate (SDS), an anionic surfactant that could enhance particle growth, coagulation and flocculation will be used for Al_2O_3 nanoparticles synthesis and applied for the demetallization of nickel from crude oil [11]. In this report, the monitoring of removal efficiency of total sample filtrate from each adsorption process with Atomic Absorption Spectrophotometry (AAS) in place of UV-Vis will also be reported.

Materials and Methods

All the reagents used were of analytical grade. Aluminum Chloride hexahydrate ($AlCl_3.6H_2O$), Sodium hydroxide, (NaOH), Sodium dodecyl sulphate (SDS), triethanolamine (TEA) and ethanol (C_2H_5OH) were all purchased from Aldrich. Almost all the reagents were used as received without further purification except SDS that underwent conductivity test to verify its purity using the value of its critical micelle concentration (CMC). The reagents used for crude oil digestion were potassium permanganate ($KMnO_4$) and conc. (HCl, HNO_3 and H_2SO_4). The crude oil sample was collected with amber bottle (to avoid light interaction) from Qua-Ibo Ocean Terminal Location, SBMI, AkwaIbom State of Nigeria on the 5thof July, 2015 and brought to Chemistry laboratory.

Synthesis of Al_2O_3-SDS and Al_2O_3 nanoparticles

A modified Cabrera [9] method was used in the synthesis of the aluminum oxide, Al_2O_3 nanoparticles (sample) according to the following steps: (i) A 5.0 ml solution containing 1.0 g (25 mmol) of sodium hydroxide in deionized water was added to 20 ml of Triethanolamine (TEA). The solution was heated at 120°C for 5 min to evaporate the water. This was followed by a slow addition of 0.49 g (20 mmol) of$AlCl_3.6H_2O$ into the solution while stirring. The resulting clear solution obtained was heated at 150°C for 10 min (solution A). (ii) The second solution was prepared by dissolving 2.64 g (10 mmol) of sodium dodecyl sulphate in 20 ml of water at 60°C (solution B) (iii) Solution A was gradually added to solution B with continuous stirring at 60°C. The mixture was allowed to age for 72 h to give a white suspension (solution C). Solution C was filtered and the residue (white solid) obtained from the mixture was washed with ethanol and allowed to dry at 30°C. The synthesized Al_2O_3+SDS were calcined in air at 550°C for 5 h in a muffle furnace. The modifications involved the use of $AlCl_3.6H_2O$ and SDS in place of Al *sec*-butoxide and cetyltrimethylammonium bromide (CTAB), respectively. The control sample, Al_2O_3 was synthesized using the same procedure without SDS.

Characterization (XRD, SEM and EDS): The X-ray diffraction (XRD) analysis of the samples was performed with the Mini-flex Rigaku XRD model equipped with PC-APD diffraction software. The operator could only generate indexed spectra images not text files. The radiation source was Cu K∝ (λ=1.54 Å). The 2θangle range selected was 6-84° with a step size of 0.02 for 0.25 s per step. Particle size estimations were evaluated according to Scherrer's equation [5]. Few powder particles of the samples were placed on conductive carbon sticky pads with a spatula and gummed unto aluminum stubs for Scanning Electron Microscopy (SEM) analysis. The SEM used was Hitachi model 5.5500 integrated with Energy Dispersive X-ray Spectroscope (EDS).

Pretreatment of the crude oil: (acid digestion)/AAS analysis: Determination of metal contents of Qua-Ibo crude oil was done using the AA500 (PG INSTRUMENTS) AAS model. Samples for AAS analysis were subjected to pretreatment. This involved the oxidation of 1.0 g of homogenized crude sample (analyte) with 1.0 g of potassium permanganate powder in a beaker. Thereafter, 1.0 ml of conc. H_2SO_4 was then added to the mixture. A strong exothermic reaction was observed as the crude oil matrix oxidized with evolution of gases. The beaker and its content were allowed to cool, then 2 ml of conc. HNO_3 and 10 ml of conc. HCl were added, and the mixture heated until there was no more evolution of toxic gases at temperatures below 150°C to avoid volatilization. The mixture was filtered and the filtrate heated to drive off excess HCl. The resulting solution was then transferred to a 100 ml volumetric flask and the volume made up with distilled water. A 0.6 mg of the analyte solution was aspirated into the AAS machine for metal (nickel) content determination.

Batch adsorption studies

The synthesized Al_2O_3+SDS and Al_2O_3 were applied in the adsorption of metal ions (Ni^{2+}) from the crude oil sample using the batch adsorption method using a mechanical shaker set at 300 rpm. The factors influencing the kinetics of (Ni^{2+}) removal by Al_2O_3 with and without SDS were investigated. Such factors include agitation time (contact time), adsorbent concentrations (Al_2O_3+SDS and Al_2O_3), and initial Ni^{2+} ion concentration (adsorbate\crude oil concentration).

Effect of agitation time: The agitation time was investigated separately for both samples at different time intervals of 5, 30, 60, 90 and 120 min at constant adsorbent concentration (0.1 g). The total volume of the solution used was 20 ml comprising of a 5:15 ratio of water/crude oil. It was mechanically shaken at 300 rpm.

Effect of adsorbent concentration (Al_2O_3 dosage): The effect of adsorbent was carried out at different concentrations of 0.02, 0.04, 0.06, 0.08 and 0.10 g of each adsorbent (Al_2O_3+SDS and Al_2O_3 respectively) using the same water - crude oil sample of 5:15 v/v respectively.

Effect of initial Nickel (Ni^{2+}) ion concentration (crude oil\ adsorbate dose): The effect of adsorbate concentration (volume of crude oil) on sorption of Ni^{2+} ion was studied at constant weight (0.10 g) of the adsorbent with varying ratios of crude oil to water as 5:15, 10:10 and 15:5 ml respectively at an agitation time of 2 h. The resulting mixture of oil/H_2O/sample was left to stand for 24 h in order to facilitate the separation of the different layers. The water was carefully separated from the crude oil layer and the crude oil analyzed for the Ni^{2+} ion after acid digestion. The amount of Ni^{2+}ion remaining in the crude oil was determined and used in the calculation of percentage removal (% R) as shown in eqns. (1).

$$\%R = \frac{C_{initial} - C_{final}}{C_{initial}} \times 100 \qquad (1)$$

Where $C_{initial}$ and C_{final} are initial and final concentrations of nickel ions (μg/ml) respectively.

Adsorption kinetics

The demetallization of nickel ion by the synthesized Al_2O_3

nanoparticles with and without SDS was studied using the pseudo first (Lagergren) and second order kinetics as expressed in eqns. (2) and (3) respectively

$$\ln\left(q_{e-}q_t\right) = lnq_e - K_1 t \quad (2)$$

$$\frac{t}{q_t} = \left(\frac{1}{K_2 q_e^2}\right) + \frac{1}{q_e} \quad (3)$$

From eqns. (1), q_e and q_t represent the amount of Ni^{2+}adsorbed by the nanoparticles (mg/g) at equilibrium and at any time t (min) respectively, K_1 (Min^{-1}) is the rate constant of the pseudo- first –order. A linear plot of ln (q_e-q_t) against t (time) produce a slope for the evaluation of the rate constant, K_1 while the correlation coefficient R^2 values were generated from data with excel software. In eqns. (2) (pseudo-second–order), K_2 (g/mg/min) is the rate constant of adsorption, q_e and q_t are the amounts (mg/g) adsorbed at equilibrium and at any time t respectively. The equilibrium adsorption capacity (q_e) and the pseudo-second order rate constants (K_2) were calculated from the slope and intercept of the linear plot of t/qt against t respectively.

Adsorption isotherms

Adsorption isotherm studies are important in the design of adsorption process as they determine the efficiency of adsorption processes [12]. Langmuir and Freundlich Isotherms were used.

Langmuir: The maximum adsorption capacity corresponding to complete monolayer coverage on the adsorbent surface is expressed by Langmuir isotherm shown in eqns. (4).

$$\frac{Ce}{qe} = \frac{KL}{qmax} + \frac{1}{qmax}Ce \quad (4)$$

Where q_{max} is the maximum adsorption at monolayer (mg/g) Ce is the equilibrium concentration of metal ion, q_e is the amount of ion adsorbed per unit weight and K_L is the Langmuir constant which is related to the affinity of binding sites (mgL^{-1}). A linear plot of Ce/q_e against Ce gives 1\$q_{max}$as slope and K_L\$q_{max}$ as intercept from where the values of q_{max}, and K_L will be calculated.

Freundlich: The Freundlich adsorption model (eqns. (5)) explains adsorption due to multilayer and heterogeneous surfaces.

$$logq_e = logK_f + \frac{1}{n}logC_e \quad (5)$$

K_f and n are called Frenundlich constants and defined as relative adsorption capacity and intensity of sorption process respectively. A plot of logq_e Vs Ce gives log$K_f$as intercept and n as slope. The correlation coefficient R^2 and the Freundlich parameters are also shown in tables.

Results and Discussion

X-ray diffraction analysis of Al_2O_3-SDS and Al_2O_3

The XRD patterns as indexed with the PC-APD diffraction software showed sharper peaks with fewer bauxite and silica impurities for the Al_2O_3+SDS compared to those of Al_2O_3 (Figure 1). This implied that the carbonization of the SDS helped to reduce impurity phases in Al_2O_3+SDS. The estimated particle sizes were calculated as 197 and 183 nm for Al_2O_3+SDS and Al_2O_3 respectively from Sherrers equation using their full width at half maximum data. Broader peaks are associated with smaller particles, which are harder for X-ray penetration, and this agreed with the results of Figure 1.

SEM and EDS

The surface morphologies of the Al_2O_3+SDS and Al_2O_3 nanoparticles

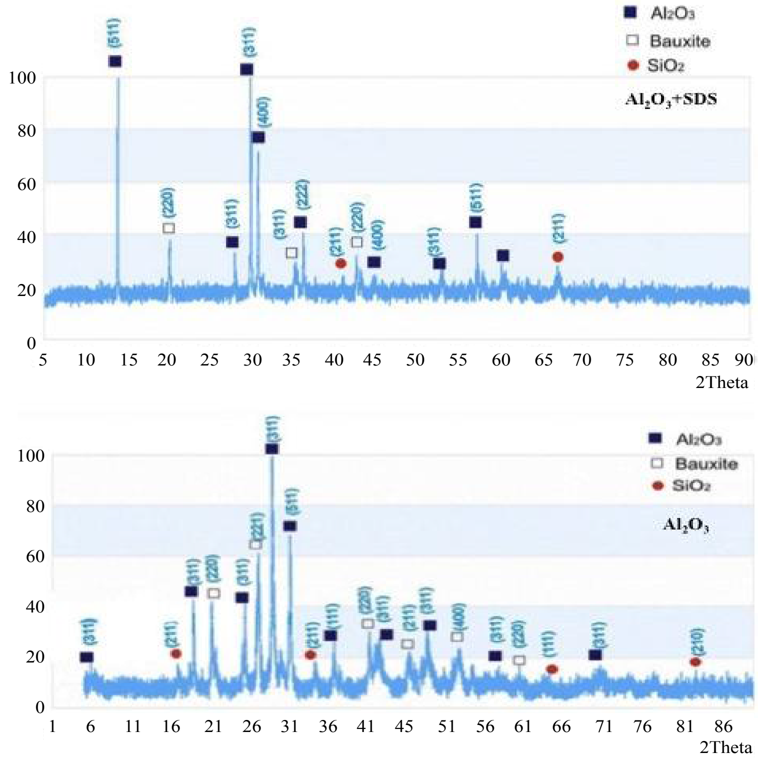

Figure 1: XRD of Al_2O_3+SDS and Al_2O_3 showing indexed peaks of Al_2O_3 with minor impurities of silica (SiO_2) and bauxite ($Al_2O_3.H_2O$).

Citation: Konne LJ, Iheanetu UD, Cookey AG (2017) Demetallization of Nickel from Crude Oil using Aluminum Oxide (Al_2O_3) Nanoparticles Synthesized with Sodium Dodecyl Sulfate (SDS). J Material Sci Eng 6: 385. doi: 10.4172/2169-0022.1000385

analyzed using SEM are shown in Figure 2a and 2b respectively while their respective images containing the EDS data are also shown in Figure 2c and 2d. Al_2O_3+SDS (Figure 2a and 2c) appear as organized rectangular polycrystallite plates with wider pores while the Al_2O_3 (Figure 2b and 2d) reveal a rough porous thinner plate-like morphology which appear net-like in Figure 2d. The polycrystallites size variation patterns agreed with the XRD estimated values. The EDS on Figure 2c and 2d confirmed the major constituent elements of Al and O with higher percentages among common impurities of Mn, Fe, and Si also found on other samples analyzed with the same instrument. The missing O on Figure 2c was shown on a repeated spectrum but its image was blurred and so was not used.

The effect of agitation time

The calculated %R (eqns. (1)) showed a gradual increase with time from 5 min (near zero) to 90 min and a sharp increase from the 90th to its maximum of 94% at 120th min for Al_2O_3+SDS. This implied that the active adsorption sites were not saturated at 120 min. On the other hand, an undulating pattern was observed with the control (Al_2O_3) with its maximum %R at the 90th min. The significant gap (difference) between the two patterns can be linked to increase in surface area created by the presence of SDS (Figure 3a) thus achieving the desired adsorptive capacity enhancement. The importance of the shaking/agitation time comes from the need for identification of the possible rapidness of binding and removal process of the Ni^{2+} from crude oil [13].

The effect of adsorbent (Al_2O_3) and adsorbate (crude oil) concentrations

The effect of adsorbent dosage on Ni^{2+}removal at different

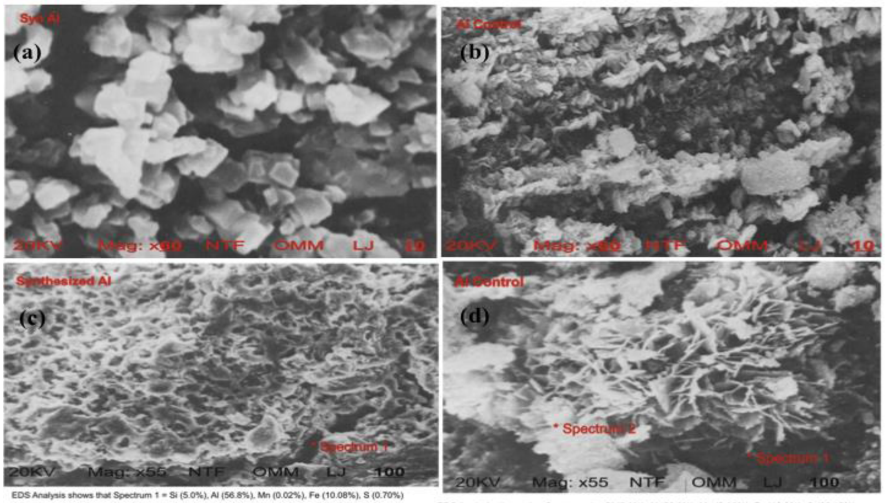

EDS Analysis shows that Spectrum 1 = Si (5.0%), Al (56.8%), Mn (0.02%), Fe (10.08%), S (0.70%)

EDS Analysis shows that Spectrum 1 = Si (5.6%), Al (56.8%), Mn (0.02%), Fe (10.0%), O (22.15%)

Figure 2: SEM of (a) Al_2O_3+SDS; (b) Al_2O_3 and their corresponding EDS (c) and (d) respectively.

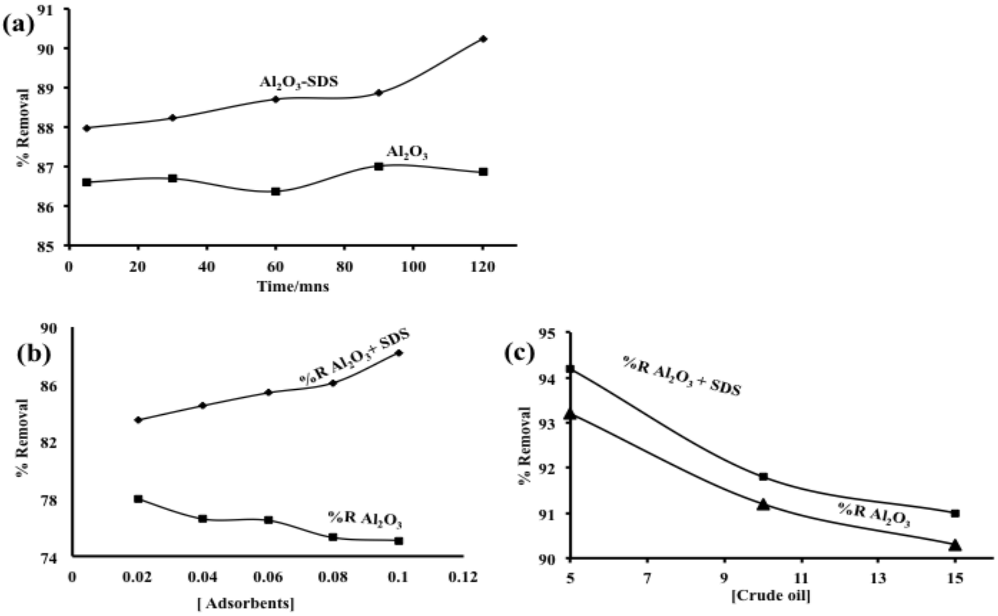

Figure 3: %Removal vs. (a) Agitation time, (b) Adsorbent and (c) Adsorbate (Crude oil) concentrations.

dosages of Al_2O_3+SDS (0.02, 0.04, 0.06, 0.08 and 0.1 g) showed that %R that increase gradually with increase in adsorbent from 0.02 to 0.1 g to a maximum at 86.1%. This implied that more active sites were introduced with increase in adsorbent concentration becoming more rapid towards the maximum concentration used (Figure 3b). However, there was a decline with increase in concentration of the adsorbent in the case of the control (Al_2O_3) giving maximum %R of 78% at the least (0.02 g) dosage (Figure 3b). This implied that equilibrium was reached quickly at 0.02 g such that additional adsorbent dosage crowded some of the available sites thereby reducing the adsorption capacity rather than enhancement.

Also the removal efficiency of Ni^{2+} by the adsorbents at varying adsorbate (crude oil) concentrations as investigated is shown in Figure 3c. It was observed that there was rapid decline in adsorption with increase in adsorbate (crude oil/Ni^{2+}ion) concentrations with both samples (Al_2O_3+SDS) and the control (Al_2O_3) respectively. However, the former adsorbent still gapped the latter with 1%. The adsorbents active sites become quickly saturated with Ni^{2+} ions and equilibrium is reached such that additional crude oil (Ni^{2+} ion) merely increases the analyte concentration.

The effect of adsorbent (Al_2O_3) and adsorbate (crude oil) concentrations

The effect of adsorbent dosage on Ni^{2+}removal at different dosages of Al_2O_3+SDS (0.02, 0.04, 0.06, 0.08 and 0.1 g) showed that %R that increase gradually with increase in adsorbent from 0.02 to 0.1 g to a maximum at 86.1%. This implied that more active sites were introduced with increase in adsorbent concentration becoming more rapid towards the maximum concentration used (Figure 3b). However, there was a decline with increase in concentration of the adsorbent in the case of the control (Al_2O_3) giving maximum %R of 78% at the least (0.02 g) dosage (Figure 3b). This implied that equilibrium was reached quickly at 0.02 g such that additional adsorbent dosage crowded some of the available sites thereby reducing the adsorption capacity rather than enhancement.

Also the removal efficiency of Ni^{2+} by the adsorbents at varying adsorbate (crude oil) concentrations as investigated is shown in Figure 3c. It was observed that there was rapid decline in adsorption with increase in adsorbate (crude oil/Ni^{2+}ion) concentrations with both samples (Al_2O_3+SDS) and the control (Al_2O_3) respectively. However, the former adsorbent still gapped the latter with 1%. The adsorbents active sites become quickly saturated with Ni^{2+} ions and equilibrium is reached such additional crude oil (Ni^{2+} ion) merely increase the analyte concentration.

Adsorption kinetics

The Pseudo-first-order plot of the adsorption of Al_2O_3+SDS and Al_2O_3 plots are shown in Figure 4a and 4b respectively. The graphs showed a poor linear relationship of ln (qe-qt) against t with both processes achieving a maximum at 60 min. The non-linearity of these plots showed that a first-order mechanism was not followed in this process. The adsorption first-order mechanism for Al_2O_3+SDS showed a steady rise that climaxed at 60 with a slight decline to the 120th min while an undulating or wave-like curve was observed for Al_2O_3. However, the linearity of the second-order plots of both samples (Al_2O_3+SDS and Al_2O_3) as shown in Figure 4c and 4d confirmed that the process followed the kinetic second-order mechanism.

See higher correlation coefficient (r^2) for the second-order mechanism against those of Lagergren in Table 1. This result agreed with similar reports of better fits of adsorption processes of metal ions to pseudo-2nd-order model in literature [14,15]. While the adsorption

Pseudo-1st-Order	q_e (mg/g)	K_1 min^{-1}	r^2
0.1g Al_2O_3+SDS	0.000098	-0.1078	0.6735
0.1g Al_2O_3	5689	0.0002	0.2755
Pseudo-2nd-order	qe (mg/g)	K_2 min^{-1}	r^2
Al_2O_3+SDS	0.2156	44.77	0.9999
Al_2O_3	0.2235	7.865	0.9998

Table 1: Pseudo-1st-Order and Pseudo-2nd-Order mechanism constants/correlation factors.

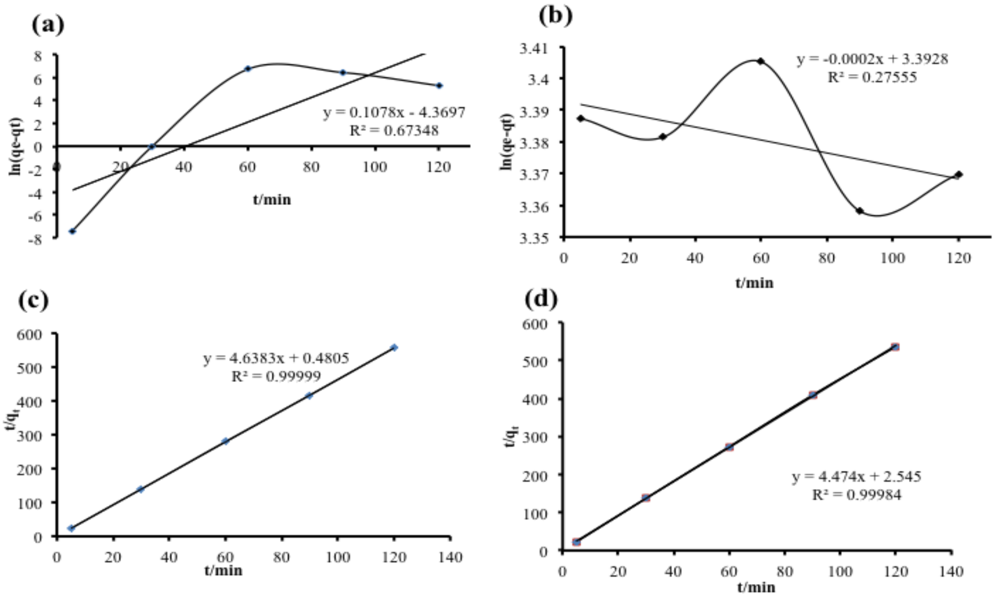

Figure 4: Plots of (a and b) Pseudo-First-Order (Lagergren) and (c and d) Pseudo-Second-Order models.

Citation: Konne LJ, Iheanetu UD, Cookey AG (2017) Demetallization of Nickel from Crude Oil using Aluminum Oxide (Al_2O_3) Nanoparticles Synthesized with Sodium Dodecyl Sulfate (SDS). J Material Sci Eng 6: 385. doi: 10.4172/2169-0022.1000385

capacity at equilibrium, qe (mg/g) was higher for Al_2O_3 in both mechanisms; K_2 of Al_2O_3+SDS process was better.

Adsorption isotherm

A plot of Ce/qe against Ce of both samples according to the Langmuir isotherm (eqns. (4)) is shown in Figure 5a and 5b for Al_2O_3+SDS and Al_2O_3 respectively. The former showed better correlation over the latter. This means that Al_2O_3+SDS data fitted the Langmuir model better. This happens when there is more homogeneous distribution of active sites leading to complete coverage of the surface by a monolayer of adsorbate. The Langmuir model also assumes that the energies of adsorptions were uniform and independent of the surface coverage. A characteristic Langmuir isotherm dimensionless constant of separation factor (R_L) used to verify the favourability of an adsorption process by adsorbents is shown in eqns. (6) and the evaluated values in Table 2.

$$R_L = \frac{1}{K_{L+C_o}} \tag{6}$$

where K_L is the Langmuir constant, C_o is the initial concentration of the nickel ion (Ni^{2+}). The R_L value expresses the shape of the isotherm [10]. If R_L value is $0<R_L<1$, it indicates favorable adsorption, $R_L>1$ shows unfavorable adsorption. $R_L=1$ indicate linear adsorption and $R_L=0$ indicates irreversible adsorption isotherm respectively. The R_L values >0 obtained for both adsorbents (Al_2O_3+SDS and Al_2O_3) confirmed favourable adsorption process. The slope of the tangent to the plot of Ce/qe against Ce gave the qmax and K_L respectively (Table 2).

The equilibrium data fitted to the Freundlich isotherm (eqns. (5)) can be used to describe a non-ideal adsorption or adsorption due to multilayer or heterogeneous surfaces. Figure 5c and 5d showed the Freundlich plots for the Al_2O_3+SDS and Al_2O_3 adsorbents respectively with the constants in Table 2. The values of n for well-fitted Freundlich isotherm should lie between 1 and10 but the values for the both adsorbents were below 1 [16]. Adsorption capacity, K_f of Al_2O_3+SDS was over fifty thousand times higher than that of Al_2O_3 as shown in Table 2. The lower correlation factors, r^2 compared to Langmuir suggested poorer fitting for Freundlich.

This is because Langmuir model has higher correlation coefficients of 0.95712 and 0.95258 while Freundlich, 0.8490 and 0.8079 for Al_2O_3-SDS and Al_2O_3 respectively. Also it has favourable dimensionless constant R_L indicating a monolayer adsorption process.

Conclusion

The sol-gel synthesis of Al_2O_3 with sodium dodecyl sulphate (Al_2O_3+SDS) and Al_2O_3 and their application in demetallization of nickel ions from crude oil-water mixtures has been reported for the first time. The XRD confirmed that both samples contained Al_2O_3 as the major phase with some minor impurities of bauxite and silica. Particle size estimations for both samples gave 197 and 183 nm respectively. This size variation was supported by the SEM micrographs that showed larger rectangular porous crystallites and thinner net-like-vertical platy crystallites for the former and later samples respectively while the EDS confirmed the presence of Al and O elements. %R of the adsorption process increase gradually with increase in adsorbent from 0.02 to 0.1 g to a maximum at 86.1% for the Al_2O_3+SDS but decrease with increase in concentration of the adsorbent in the case of the control (Al_2O_3) with an %R maximum of 78% at the least (0.02 g) dosage. Higher removal efficiencies of 94 and 93% for a 1:3 crude oil-water mixture were also recorded for Al_2O_3+SDS and Al_2O_3 at constant adsorbate

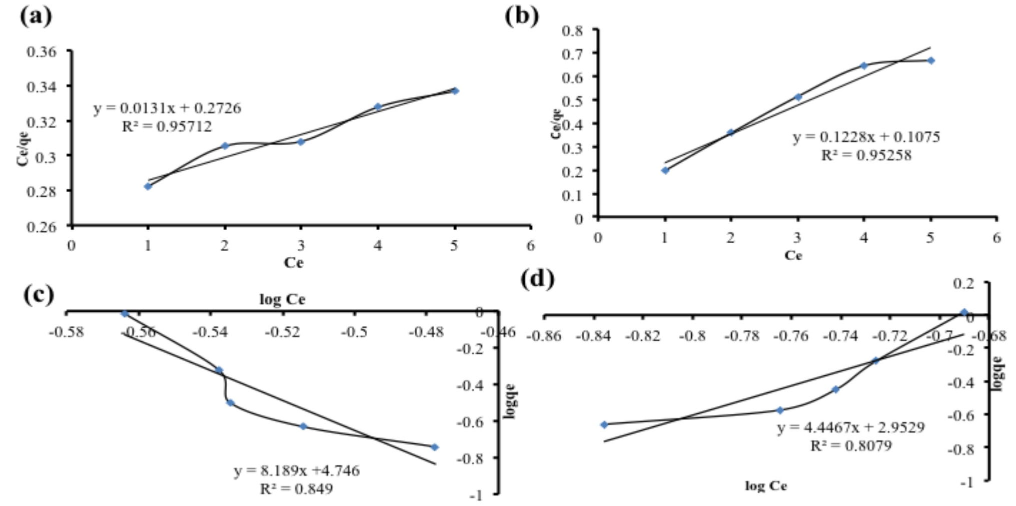

Figure 5: Plots of log agitation time vs. (a) log [Al_2O_3+SDS]; (b) [Al_2O_3] (Langmuir) and logq_e vs. logCe of (c) Al_2O_3+SDS; (d) Al_2O_3 (Freundlich).

Adsorbents	Langmuir parameters			
	q_{max} (mg/g)	K_L (L/mg)	R^2	R_L
Al_2O_3+SDS	76.34	20.809	0.95712	0.0373
Al_2O_3	8.143	0.875	0.95258	0.4796
	Freundlich Parameters			
	K_f (mg/g)	N	R^2	
Al_2O_3+SDS	55718.57	0.1221	0.849	
Al_2O_3	897.22	0.2249	0.8079	

Table 2: Langmuir and Freundlich isotherm parameters and correlation coefficients.

concentrations, respectively. The kinetic study confirmed that Ni^{2+} demetallization followed pseudo-second-order model. Demetallization of the Ni^{2+} by Al_2O_3 was also favored by the presence of SDS surfactant, contact time, concentration of the synthesized Al_2O_3 nanoparticle and the adsorbate (crude oil/Ni^{2+}) concentration. The adsorption isotherms showed better fits to the Langmuir model. Adsorption of (Ni^{2+}) by Al_2O_3+SDS gave higher adsorption capacity than Al_2O_3 and its recommended for demetallization processes in the oil industry.

Acknowledgements

Authors wish to acknowledge Mr. Collins Ofiwe of the Centre of Nanotechnology and Advanced Materials, Engineering Development Institute (EMDI), Akure, Ondo State for the SEM and XRD analysis and Getamme Laboratories Nigeria Ltd Port Harcourt for AAS. The authors declare that there is no conflict of interest concerning this publication.

References

1. Odularu GO (2008) Crude Oil and the Nigerian Economy Performance. Oil and Gas Business 1-29.
2. United Nations Environment Programme (UNEP) Report (2011).
3. Onojake MC, Oforka NCO, Suji LC (2011) Trace Metals Geochemistry of Crude Oils from Umutu/Bomu Fields in South West Niger Delta Nigeria. Energy and Environment Research 1: 139-146.
4. Duyck C, Miekeley N, Porto da Silveira CL, Aucélio RQ, Campos RC, et al. (2007) The determination of trace elements in oil and its heavy fractions by atomic spectrometry. Spectrochimica Acta Part B 62: 939-951.
5. Konne JL, Opara K (2014) Remediation of Nickel from crude oil obtained from Bomu Oil Field using cassava waste water starch stabilized magnetic nanoparticles. Energy and Environment Research 4: 25-31.
6. Reynolds JG (2004) Removal of nickel and vanadium from heavy crude oils by exchange reactions. Prepr Pap Am Chem Soc Div Fuel Chem 49: 79.
7. Wen Z, Yang L, Xu X, Gao J (2013) Removal of Nickel and Vanadium from Crude oil by Microwave-Chemical Method. Petroleum Science and Technology 31: 991-999.
8. Nassar NN (2010) Asphaltene Adsorption onto Alumina nanoparticles: Kinetics and Thermodynamics Studies. Am Chem Soc 24: 4116-4122.
9. Cabrera S, Haskouri JE, Alamo J, Beltrán A, Beltrán D, et al. (1999) Surfactant-Assisted Synthesis of Mesoporous Alumina Showing Continuously Adjustable pore sizes. Advanced Materials 11: 379-381.
10. Abbas A, Mohammad ST, Hassan B (2010) Simultaneous removal of heavy-metal ions in wastewater samples using nano-alumina modified with 2, 4-dinitropheny / hydrazine. Hazardous Materials 181: 836-844.
11. Imtiaz A, Muhammad A, Muhammad K, Rohana A (2013) Micelle-Assisted Synthesis of Al_2O_3.CaO Nanocalalyst: Optical properties and their Applications in Photo degradation of 2, 4, 6-Trinitrophenol. The Scientific World Journal pp: 1-11.
12. Mohammed AM (2015) Kinetics and thermodynamics of aluminium oxide nanopowder as adsorbent for Fe (III) from aqueous solution. Basic and Applied Sciences 4: 142-149.
13. Farghali AA, Bahgat M, Allah AE, Khedr MH (2013) Adsorption of Pb(II) ions from aqueous solutions using copper oxide nanostructures. Journal of Basic and Applied Sciences 2: 61-70.
14. Bhattacharya AK, Mandal SN, Das SK (2006) Adsorption of Zn (II) from aqueous solution by using different adsorbents. Chem Eng J 123: 43-51.
15. Bhattacharya AK, Naiya TK, Mandal SN, Das SK (2008) Adsorption, kinetics and equilibrium studies on removal of Cr (VI) from aqueous solution by using different low-cost adsorbents. Chem Eng J 137: 529-541.
16. Dada AO, Olalekan AP, Olatunya AM, Dada O (2012) Langmuir, Freundlich, Tempkin and Dubinin-Radushkevich Isotherms Studies of Equilibrium Sorption of Zn^{2+} Unto Phosphoric Acid Modified Rice Husk. J Appl chem 3: 38-45.